

# Sensing-Aided Scalable Peer-to-Peer Millimeter-Wave Communication

Sidong Guo, Shez Malik, Xiangyu Li

*School of Electrical and Computer Engineering, Georgia Institute of Technology, Atlanta, United States*

E-mails: {sguo93, smalik46, xli985}@gatech.edu

**Abstract**—One of the bottlenecks of modern communication is to enable sensing and communication simultaneously with causing scheduling conflicts, and how sensing may be leveraged to help directional communication accuracy. To this end, we propose and implement a novel peer-to-peer mmWave communication system to achieve joint beamforming and sensing. A radar and IMU assisted tracking and beamforming algorithm is designed and tested and the results show robust tracking capacity with an overall higher throughput obtained. The results demonstrated promising future extensions where with refinements the design and implementation can be deployed in a more scalable manner.

**Index Terms**—millimeter-wave, sensing, beamforming, mobility, Kalman Filtering

## I. INTRODUCTION

Recent years have witnessed an increasing demand for high data rates in support of wireless communications among groups of user equipments (UEs). One of the promising 5G and beyond wireless technology is Millimeter-wave (mmWave) communications, which is stimulated by the global spectrum shortage from the previous 2G frequencies to present 5G frequencies [1], is attracting significant attention because of its huge amounts of spectrum, high propagation gain and other particular channel spatial features [2]. Motivated by its advantage, the efficiency and QoS can be further increased by enabling efficient client to client communication. Moreover, further improvements to the mmWave communication systems in terms of accuracy, mobility, and reliability can be obtained by integrating mmWave communications with sensing and beamforming technologies for the orientation, localization, and data transmission of clients in the desired range.

Next-generation communications will rely heavily on sensors, including radars, lidars, and cameras [3] for services with higher quality and efficiency. By leveraging these sensing technologies before the data transmission stage, the real locations of clients in need of mutual communications can be obtained [4] and continuous detection and tracking is achievable in a real-time manner. These will make the best use of energy for transmitting data, especially when directionality is a required condition for effective mmWave beamforming [5], largely avoid energy consumption wastage and reach the goal of green communications.

This research project is partly supported by the Mobile Advanced Research group at GATech (MARGA).

## A. Related Work

Using mmWave for sensing related purposes has been studied extensively in the past. A case of using mmWave bands for enhanced local area (eLA) access in 5G is studied by Ghosh *et al* [6]. In this eLA system, peak data rates of more than 10 Gbps and edge data rates in excess of 100 Mbps can be achieved with huge bandwidth of mmWave. It is also demonstrated that in mmWave-supported cellular access networks, higher coverage and capacity are likely to be obtained [7] [8]. With directional antennas, capacity gains, power, and spectral efficiency can be largely improved in the potential device-to-device (D2D) communications [9].

For indoor scenarios of mmWave communications, schemes with different settings were investigated to improve the QoS. In [1], the spatial modulation multiple-input-multiple-output (MIMO)-based scheme in indoor line-of-sight (LOS) mmWave communication at 60 GHz is investigated. In the theoretical aspect, the error performance of spatial modulation is optimized by maximizing the minimum Euclidean distance of received symbols. However, due to the directionality of mmWave, the location and orientation of target clients are required for higher accuracy. Sensing technology using radar can greatly assist this imperfection. The survey [4] introduces an approach for indoor detection and tracking of humans using mmWave sensor, where no mutual communications are required for further error correction. In [2], a radar sensing-assisted mmWave communication scheme is designed, but the results are obtained in a two-dimensional (2-D) environment via simulation while no field tests are conducted. In addition, beamforming in mmWave communications is also deeply discussed based on its large bandwidth, unique channel features and hardware constraints in [10]. The precision of beamforming direction will dictate the effective throughput during peer-to-peer communications.

While many of the aforementioned works have been brought by providing schemes and simulation of performance analysis for mmWave communications, few have been made achievable in practical life. These have brought about the need for a real-world design and implementation of peer-to-peer communications under an appropriate combination of mmWave utilization and related sensing-aided technologies.

## B. Motivation and Challenge

Motivated by these existing works, this research selects three MikroTik wAP 60G AP routers as an access point (AP)

and clients in support for 60 GHz mutual communications, one Retina 4SN for the 60 GHz sensing technology, and two MPU9250 GY-9250 devices for IMU data collection and transmission. Two Raspberry Pi 3 (RPI) are employed for upper-layer control over information and data exchange among routers. However, due to the inherent characteristics of mmWave and practical environments, there are three main challenges that we need to overcome.

(1) Scheduling. Joint sensing and communication require a real time update on both client location and mutual communication, which takes a toll on hardware and software implementations.

(2) Directionality. During dynamic location changing of clients, the beam directions need to be calibrated in real-time in order to beamform to AP to get orientation at each client and accurately beamform between clients to realize inter-communications.

(3) Noise elimination. Radar suffers from its blind estimation nature. The background noise and unrelated objects should be filtered from the desired objects to prevent incorrect target tracking.

### C. Approach and Contribution

Considering the above challenges and existing research, this paper investigates and proposes a comprehensive scheme of peer-to-peer mmWave communications for dynamic clients assisted by sensing technologies. To the best of our knowledge, we are the first to simultaneously design and implement this type of system for indoor peer-to-peer mmWave communications. The approaches for the system realization as well as the main contributions of this paper are summarized as follows.

(1) A novel system that enables peer-to-peer mmWave communications with dynamic clients and sensing technologies is deployed.

(2) An algorithm is proposed to achieve real time joint communication and sensing, as well as peer to peer beamforming of mobile clients with appreciable accuracy.

(3) We have implemented the system in lab environment and tested its performance with concrete results.

## II. DESIGN

### A. Design Overview

**Frame-based Operation.** We employ a system that operates on a frame-to-frame basis. During each frame, the radar module runs for  $n$  seconds. We extract the data corresponding to the second to last time instance for guaranteed completeness and real-time of the radar data. During the same frame, the latest IMU data is obtained from two clients and fed into the algorithm as well.

**Algorithm Flow.** Each frame of the algorithm runs around the data extracted. The radar data is passed through a tracking algorithm that calculates all clusters in view and their corresponding velocity. IMU data is used to correct and offset clients' true velocities. The cluster update algorithm is used for continuous tracking and update of clusters, after point clouds are collected with density-based spatial clustering of applications with noise (DBSCAN). The clients are identified

by comparing cluster velocity with corrected IMU velocity and the recursive Kalman Filtering is leveraged to smooth the trajectory of moving clients to ensure the realization of client mobility. With the obtained location and orientation of mobile clients, the beamforming angle can be adjusted automatically in real-time to achieve directional communication among clients

### B. Cluster Localization

**Cluster Filtering** The radar data returns a collection of point clouds and density-based spatial clustering of applications with noise (DBSCAN) with empirically-selected hyper-parameters,  $Eps = 0.3, N = 100$ , which is applied to identify all the clusters and filter out noise clusters. After this, a second layer of filter is applied whereby all clusters with strictly zero doppler are regarded as background objects and filtered out, with the key observation being that even a stationary client has non-zero points.

**Cluster Update** All remaining clusters are represented by corresponding core points calculated as centroids. During each frame, and beginning with the second frame, each cluster is mapped to its most likely cluster counterpart of the current frame. This is accomplished with the following algorithm.

---

#### Algorithm 1 Cluster Update Algorithm

---

**Input:** A list of clusters from current frame,  $C$

**Input:** A list of clusters from previous frame,  $C_p$

**Input:** Threshold =  $T$

**Output:** A list of clusters from current frame in  $C_p, C_c$

---

```

if  $|C_p| == 0$  then
     $C_c = C$ 
else
    if  $|C_p| \leq |C|$  then
         $C_c = MLE(C_p)$ 
    else
         $C_c = MLE(C)$ 
    end if
    if  $|C_c(\text{cluster}A) - C_p(\text{cluster}A)| \geq T$  then
        Delete clusterA
    end if
end if

```

---

In the algorithm above, the Maximum Likelihood Estimator (MLE) is calculated in the following way:

$$C_c = \underset{C_c \in \mathbb{C}^{\min(|C_p|, |C|)}}{\operatorname{argmin}} \|C_c - C_p\| \quad (1)$$

where  $|C|$  means the cardinality of the set  $C$ , and  $\mathbb{C}$  is the space formed from current list of cluster  $C$  before matching.

The threshold in the above algorithm can be determined in the following way. Assume the client follows a random Gaussian process, in which situation we may model the velocity as a Gaussian random variable with  $v \in \mathcal{N}(v_m, v_r)$ . The threshold is picked with certain percentage confidence as several standard deviations from the mean velocity.

### C. Orientation and Velocity Tracking:

**Velocity:** We employ a very principled approach to velocity tracking. After IMU readings are calibrated, the velocity is calculated as the integral of acceleration over frame duration:

$$V_c = V_p + (A_c + A_p)/2 \cdot t \quad (2)$$

where  $V_c$ ,  $V_p$ ,  $A_c$ ,  $A_p$  are velocity and acceleration from the current and previous frame respectively, and  $t$  is the frame time. The integration is discretized by choosing the average acceleration between current and previous frame IMU readings.

**Orientation:** The orientation of the client's router is tracked with the 6D Madgwick filter, after which the velocity is corrected by the orientation to convert IMU frame velocity to global frame velocity.

### D. Client Identification:

We are now in a position to identify the clients. The main idea is to find, with maximum likelihood, the corresponding clusters in  $C_c$  that are clients, by velocity comparison. This is illustrated in the following algorithm. Note that the client

---

#### Algorithm 2 Client Identification Algorithm

---

**Input:** A list of velocity from current frame clusters,  $V_{cluster}$

**Input:** A list of Velocity of two clients,  $V_{client}$

**Output:** A list of clusters corresponding to two clients

---

**if**  $Frame < 2$  **or**  $Frame > 5$  **or**  $No\ Error$  **then**  
     *Pass*

**else**

$$\hat{V} = \underset{\hat{V} \in \mathbb{V}_{cluster}^2}{\operatorname{argmin}} \|\hat{V} - V_{client}\| \quad (3)$$

*For*  $i$  **in**  $\hat{V}$ :

*Extract Cluster Label*

**end if**

---

identification is only called from frames 2 and 5, and whenever the cluster readings produce an error, either because the client moves outside the radar viewer, or it is non-line-of-sight (NLoS). Only on the second frame can the velocity lists be populated for identification to work. And practically, in order to avoid accumulated velocity drift from IMU, clients are not being continually identified after frame 5 whose tracking relies on **Algorithm 1** Cluster Update Algorithm.

### E. Kalman Filtering:

We smooth the trajectory of clients with a Kalman Filter (KF). Two key observations here are: (1) During each frame, Kalman Filter extracts the measurement coordinate of clients by using client labels determined in client identification. This could err, when cluster update post frame 5 maps client cluster onto noise points (when client velocity is high), in which case, the client identification is run again. (2) We discretize the KF by having the average frame time as the interval. The KF is constructed based on the assumption that the clients follow Newtonian physics where the force exerted upon each client follows a Gaussian random variable.

### F. Beamforming Angle Calculation:

After the filtered positions of both clients and their respective orientations are stored, we calculate the beamforming direction, which is necessary for peer-to-peer communication. The general condition is such that the clients must be in the beamspace of each other, i.e. a 180-degree span region centering the orientation of each client. After the beam angles are calculated with simple geometry, the Tx beamforming sector can be set on Mikrotik routers.

## III. IMPLEMENTATION

### A. Networking

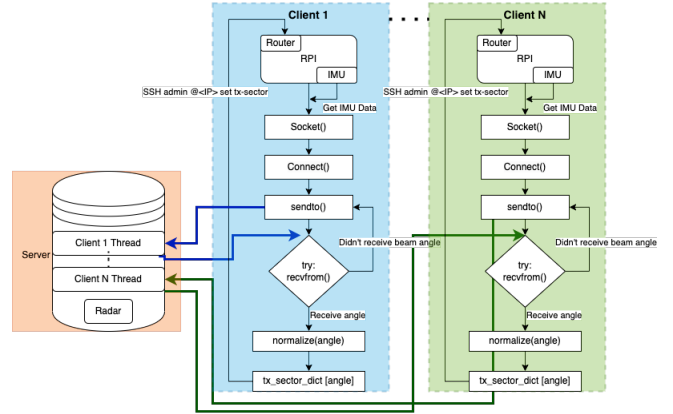


Fig. 1. IMU client back end. This flow chart describes the overall logic of the client-server communication link.

The networking aspect of the system is implemented by leveraging a multithreaded server that continuously retrieves the latest IMU data from each client (**Figure 1**). The client-to-server communication link is realized by leveraging the UDP networking protocol in which each client is bound to a unique port on the server. During each frame, a thread-safe operation transfers the data from the individual client threads to a local object whose values can be read and matched with the most recent radar data. The design decision is made to minimize latency between the received data from the IMUs and the detection data from the radars. This creates a more consistent basis upon which these nearly simultaneous data points can be analyzed by the algorithm mentioned in the previous section.

Upon localization of the clients by the algorithm and beam angle calculation, the calculated angle between both clients is then communicated back to each client respectively. Once this is accomplished, each client will determine which antenna must be used to beamform and normalize the angle according to the best antenna choice as mentioned in II-F and retrieves the tx-sector value that corresponds with the calculated angle. This allows the RPI to “Secure Shell (SSH)” onto the router’s admin user and set the tx-sector value accordingly.

### B. Hardware

**Server:** The server is composed of three MikroTik 60G routers: one single antenna router and two three-antenna routers, as well as a RETINA 4SN 60GHz Radar. This system

is set up with a Linux Desktop running Ubuntu 11.04 LTS, used to launch and run the algorithm. Each router can direct its beam to one of the many tx-sectors, which is a set of non-overlapping spatial region in its 60 by 30 radiation space.

**Clients:** The clients are each set up with an RPI running the latest version of Raspbian OS. These are each wired to a three-antenna MikroTik 60G router and an MPU9265 IMU. The clients are set up such that the routers are enclosed in a cardboard box with additional cardboard strapped over the antenna. This is to achieve some form of manual attenuation as there is no configurability over transmit power for the outdoor routers.

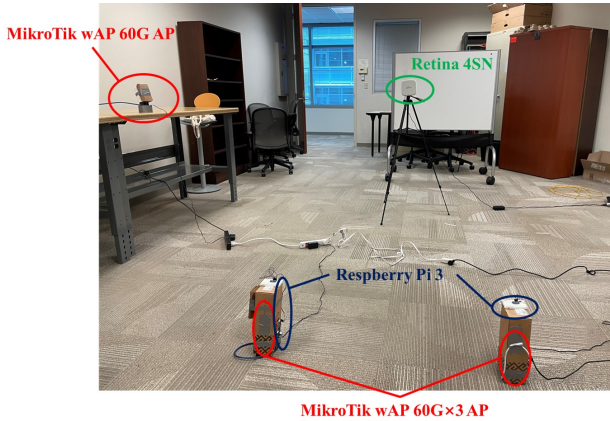


Fig. 2. General setting of related devices.

The general setting of related devices, including the server, clients, RPI and the radar can be seen in Figure 2. For the purposes of beamforming and data collection, the three-antenna routers are set to only use their middle antenna so that they would behave as a single antenna router. This is because the client routers are not capable of achieving direct communication with each other without going through the server, due to their configurations. Our results are accomplished by using our algorithm to localize the AP router which is a single-antenna router and a client router which is set to single-antenna mode. The angles are calculated accordingly and beam angles are set respectively.

### C. Testbed

This system is accomplished in an LoS environment between the radar and clients. The area is well-lit; however, lighting didn't have any implications on the radar or the algorithm's ability to track the clients. Additionally, both clients were initially still while the system stabilized and then were mobile for the remainder of the duration of tracking and beam angle calculation. The testing area is surrounded by desks as potential interference and the mobility of clients is constrained due to limited lab space.

## IV. RESULTS

### A. Tracking Accuracy

To evaluate the performance of the tracking algorithm, we follow a ground truth path Figure 3. The algorithm

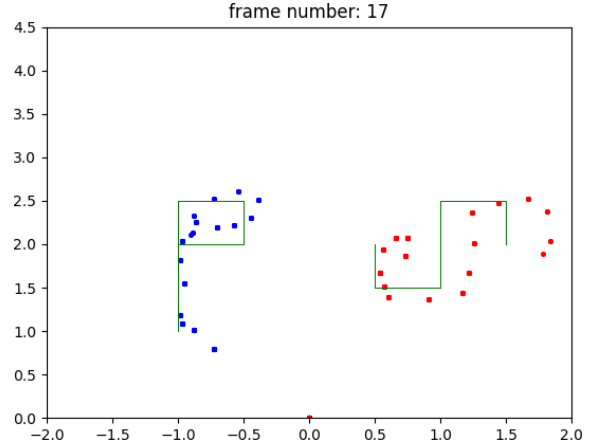


Fig. 3. The localization accuracy was evaluated with respect to a fixed ground truth pathing. The root mean square averaged over successive tests was approximately 16.24cm

dynamically tracks the clients' as they traverse the predefined path. The accuracy is calculated using the root mean square (RMS) error metric, where the true coordinate is obtained by projecting the measured coordinate onto its nearest dimension axis on the path. The RMS averaged over successive tests is approximately 16.24cm.

### B. Beamforming Performance

Beamforming performance is evaluated with respect to each intersection in the ground truth paths in the previous section (IV-A). This is then compared to the routers' own ability to beam scan. The beam scan algorithm of the routers is implemented such that multiple tx-sectors are "grouped together" and the routers slowly perform a search on each group and subgroups in between to determine which specific tx-sector value satisfies its threshold requirements for a stable connection. Once the tx-sector is determined, the received signal strength indicator (RSSI) and signal quality metrics are documented.

Similarly, for our algorithm, we allowed for the tx-sector to be calculated and set and then measured the signal quality and RSSI metrics. The signal quality metric is a transformation of signal-to-interference-plus-noise-ratio (SINR) created by MikroTik's RouterOS to provide an estimate for signal quality from 0 to 100. The results for both tests can be seen in Table I and Table II.

TABLE I  
GROUNDTRUTH RSSI VS ALGORITHM RSSI FOR EACH INTERSECTION.

Intersection	Groundtruth RSSI	Algorithm RSSI	%increase
1	-58	-53	8.62%
2	-53	-51	3.77%
3	-53	-52	1.89%
4	-55	-51	7.27%
5	-54	-55	-1.85%
6	-52	-52	0%

TABLE II  
GROUNDTRUTH SIGNAL VS ALGORITHM SIGNAL FOR EACH  
INTERSECTION. SIGNAL IS AN ARBITRARY TRANSFORMATION OF SINR  
GENERATED BY MIKROTIK'S ROUTEROS

Intersection	Groundtruth Signal	Algorithm Signal	%increase
1	85	100	17.65%
2	90	95	5.56%
3	70	95	35.71%
4	75	95	26.67%
5	100	95	-5%
6	100	95	-5%

## V. EVALUATION

### A. Tracking Accuracy

The accuracy of tracking depends largely on IMU accuracy, as a suboptimal IMU could disrupt client identification in the presence of noise or other moving objects in the environment. When the environment is clear or has relatively low noise, our tracking algorithm is very reliable. In the test area, as there are several humans in the background, it is possible for the algorithm to “lock” onto other moving objects though the algorithm is able to correct itself after a certain number of frames. The limited frame update rate means the algorithm suffers from a high-mobility environment and clients. Finally, there are two additional sources of error that could be accounted for in a further extension of the research. Firstly, the radar point clouds are only the surface of a human body, causing the the measured trajectory to drift towards radar. Secondly, eliminating elevation in core point tracking is susceptible to error if radar is not placed at an optimal height.

### B. Beamforming

The algorithm calculation of the beam angles has a cutting edge as opposed to the beam scan implementation already used by the routers. Additionally, it is important to note that because of the nature of beam scan, the RSSI and Signal Values continue to oscillate as the routers determine what the optimal tx-sector value is. These values cause the power to have a significant variance from 40 to 100 within the span of seconds. For our algorithm, this value stays more consistent and though it oscillates, it would stay from 90 to 100. This slight oscillation after algorithmically setting of the beam angle can likely be attributed to noise and interference in the environment.

Furthermore, when looking at overall performance, we can see an average of 3.3% increase in RSSI values and roughly an average of 12.6% increase for the signal metric mentioned earlier. Specifically, when looking at intersections 1, 3, and 4 we notice a significant difference in the beam scan signal and the algorithm signal. This can likely be attributed to the routers not directly facing each other and being angled from each other. While the beam scan algorithm tries to seek the best tx-sector, the variance induced in signal quality is much more drastic than the signal variance from the sensing solution that we have created.

It is also valuable to note that the range on these routers is around 500m and we were performing our experiments in a

25m<sup>2</sup> space. This implies that even if the tx-sector is incorrectly set, the RSSI values will not see significant deviations because of the transmission power of the routers themselves, even after the manual attenuation that we implemented.

## VI. CONCLUSION

In this paper, we implemented a peer-to-peer mmWave communication system assisted by mutual beamforming and radar sensing in an LOS indoor environment. We designed and completed system in all of its current capacity. The results show that the trajectories of target clients can be reliably tracked while simultaneously enabling beamforming capability. It is also evident from the results that, peer-to-peer beamforming, instead of the inefficient beamscanning, can largely improve the QoS of communications among clients. After further refinement and scale-up study, it is expected that our proposed system can be deployed in a larger enviroment, thus serving more clients simultaneously.

## ACKNOWLEDGMENT

We would like to thank Prof. Sundaresan for his instruction during the course *ECE 8803 Special Topics*, which has included all the necessary background information and knowledge to complete this project. Thanks also go to Mr. Yu-Tai Lin who has always been there for help when we are trapped by certain problems. Lastly, thank you to all the classmates with whom we have had classes and completed our projects with. It is the help from all the above that guided us in the right direction to successfully complete this project.

## REFERENCES

- [1] P. Liu, M. Di Renzo, and A. Springer, “Line-of-sight spatial modulation for indoor mmWave communication at 60 GHz,” *IEEE Transactions on Wireless Communications*, vol. 15, no. 11, pp. 7373–7389, 2016.
- [2] C. Jiao, Z. Zhang, C. Zhong, and Z. Feng, “An indoor mmwave joint radar and communication system with active channel perception,” in *Proceedings of IEEE International Conference on Communications (ICC)*, 2018, pp. 1–6.
- [3] A. Ali, N. Gonzalez-Prelcic, R. W. Heath, and A. Ghosh, “Leveraging sensing at the infrastructure for mmWave communication,” *IEEE Communications Magazine*, vol. 58, no. 7, pp. 84–89, 2020.
- [4] X. Huang, H. Cheena, A. Thomas, and J. K. Tsoi, “Indoor detection and tracking of people using mmwave sensor,” *Journal of Sensors*, vol. 2021, pp. 1–14, 2021.
- [5] Y. J. Cho, G.-Y. Suk, B. Kim, D. K. Kim, and C.-B. Chae, “RF lens-embedded antenna array for mmWave MIMO: Design and performance,” *IEEE Communications Magazine*, vol. 56, no. 7, pp. 42–48, 2018.
- [6] A. Ghosh, T. A. Thomas, M. C. Cudak, R. Ratasuk, P. Moorut, F. W. Vook, T. S. Rappaport, G. R. MacCartney, S. Sun, and S. Nie, “Millimeter-wave enhanced local area systems: A high-data-rate approach for future wireless networks,” *IEEE Journal on Selected Areas in Communications*, vol. 32, no. 6, pp. 1152–1163, 2014.
- [7] T. Bai, A. Alkhateeb, and R. W. Heath, “Coverage and capacity of millimeter-wave cellular networks,” *IEEE Communications Magazine*, vol. 52, no. 9, pp. 70–77, 2014.
- [8] T. Bai and R. W. Heath, “Coverage and rate analysis for millimeter-wave cellular networks,” *IEEE Transactions on Wireless Communications*, vol. 14, no. 2, pp. 1100–1114, 2014.
- [9] Y. Niu, Y. Li, D. Jin, L. Su, and A. V. Vasilakos, “A survey of millimeter wave communications (mmwave) for 5G: opportunities and challenges,” *Wireless networks*, vol. 21, pp. 2657–2676, 2015.
- [10] S. Kutty and D. Sen, “Beamforming for millimeter wave communications: An inclusive survey,” *IEEE communications surveys & tutorials*, vol. 18, no. 2, pp. 949–973, 2015.